Use of nano-bioglass scaffold enhanced with mesenchymal stem cells for rat calvarial bone tissue regeneration

Article · January 2014

CITATIONS
2

READS
79

5 authors, including:

Abbas Ali Imani Fooladi

257 PUBLICATIONS **2,149** CITATIONS

SEE PROFILE

Afsaneh Amiri

University of Waterloo

31 PUBLICATIONS **229** CITATIONS

SEE PROFILE

Mohammad Reza Nourani

Baqiyatallah University of Medical Sciences

136 PUBLICATIONS **1,251** CITATIONS

SEE PROFILE

Some of the authors of this publication are also working on these related projects:

Molecular O-serogrouping of Shiga toxin-producing Escherichia coli View project

Tissue engineering and regenerative medicine View project

Trends Biomater. Artif. Organs, 28(1), 8-18 (2014) *http://www.sbaoi.org/tibao*

Original Article

Use of Nano-Bioglass Scaffold Enhanced with Mesenchymal Stem Cells for Rat Calvarial Bone Tissue Regeneration

Elham Alsadat Hosseini Aghozbeni[1,2], Abbas Ali Imani Fooladi[3], Masoumeh Foroutan Koudehi[1], Afsaneh Amiri[2], Mohammad Reza Nourani[1*]

[1]*Tissue Engineering Division, Nanobiotechnology Research Center, Baqiyatallah University of Medical Sciences, Tehran, Iran.*
[2]*Department of Chemistry, Islamic Azad University, Central Tehran Branch, Tehran, Iran.*
[3]*Applied Microbiology Research Center, Baqiyatallah University of Medical Sciences, Tehran, Iran.*
*Corresponding author: r.nourani@yahoo.com

Received 6 September 2013; Accepted 1 December 2013; Available online 1 March 2014

The repair of bone defects, arising from trauma, remains a major clinical problem. Bioactive glass (BG) is a good bone scaffold, which when seeded by rat mesenchymal stem cells (rMSCs), plays a fundamental role in bone regeneration. rMSCs were isolated from the femur of rats. The nanocomposite scaffolds were prepared. In order to confirm the identity of the MSC, the proliferation medium was replaced by an osteogenic medium. The occurrence of differentiation was examined by RT – PCR analysis and alizarin red staining. Furthermore, two bilateral full-thickness defects were created in the calvarium of rats, which were then filled by scaffolds enhanced with rMSCs. To evaluate bone regeneration, histological and X-ray analyses were carried out. Following alizarin red staining, red mineralized areas appeared on the cultures. RT-PCR analysis showed the presence of osteocalcin and osteopontin receptor mRNAs in differentiated rMSCs. The present study demonstrated the ability of rMSCs to reconstruct calvarial defects in an allogenic transplantation model using BG scaffolds.

Introduction

Successful repair of severe bone defects is a major concern and an ongoing clinical challenge. In such cases, autologous bone grafting procedure is the best clinical outcome to repair bone deficiencies, based on its osteogenic and osteoinductive potential [1, 2]. However, the main disadvantages of such a procedure include potential donor site morbidity, risk of infection, and difficulty in achieving the desired bone shape and nerve damage [3]. Other bone grafting methods, such as allografts are also used, but because of their poor quality, transmission of disease from the donor to the recipient and immunogenic responses, their application has become more limited [4]. Due to these drawbacks, tissue engineering seeks to develop strategies to establish an artificial biomaterial scaffold containing regenerating competent cells.

The tissue engineered bone complex incorporates osteoconductive scaffolds, cells and osteogenic growth factors [3]. Parameters that are considered during the design and fabrication of Scaffolds from bioactive materials include degradation rate, pore size and volume [5]. Moreover, such biomaterials must be osteoconductive, with three – dimensionally interconnected pores to support cell growth, communication and bone formation [6]. Several studies, using hydroxyapatite, have reported that pore sizes larger than 350 µm lead to direct osteogenesis with enhanced vascularization [5]. Among bioactive materials, bioactive glasses are materials of choice for bone tissue engineering because they are biocompatible with soft and hard tissues, and osteoconductive materials. Also, bioactive glasses are amorphous, silicate – based materials that bond to bone and imitate new bone growth while dissolving over time [7]. Bone marrow – derived mesenchymal stem cells are adherent, non-hematopoietic cells that are capable of self –renewal, and can differentiate into several phenotypes, including bone, adipocytes and cartilage. After their isolation and extension in tissue culture,

rMSCs are capable of reconstruction bone defects upon their implantation into various animal models [8].

In addition, studies on cell–biomaterial interactions have shown that the implantation of certain progenitor cell – scaffold combinations can lead to better results in bone reconstruction, when compared to the implantation of the blank scaffolds. Mesenchymal stem cells may send out signals to recruit endothelial progenitor cells from the circulating blood, or feel signals from the microenvironment and differentiate into vascular endothelial cells. These effects are contributed to angiogenesis that is one of the important factors for bone formation and repairing [6]. In this study, the freeze drying technique was used for the fabrication of three-dimensional (3D) interconnected gelatin/bioactive glass scaffolds, which mimic both the architecture and composite nature of natural bone. Subsequently, rMSCs were seeded onto these scaffolds to evaluate the effect of the rMSC/scaffold construct on the rate of bone regeneration, as compared to that of the blank scaffold.

Materials and Methods

Preparation of nanocomposite scaffolds

Bioglass nanopowders (containing 64% SiO_2, 5% P_2O_5, and 31 % CaO) (based on mol%) was synthesized by the sol-gel technique, as described previously [9,10]. Gelatin / nano-bioglass scaffolds were fabricated, based on the freeze drying technique. Firstly, the synthesized BG nanopowder was added to a homogeneous aqueous solution of microbiology-grade gelatin (GEL) (10 % (Merck), establishing a GEL /BG composition with a respective weight ratio of 70/30. The resulting mixture was then homogenized by a stirrer at 40^0 C for 45 min. Then, layers from the homogenate were cast into plastic petri dishes and frozen at -20^0 C for 3 h. The layers were subsequently dried in a freeze drier (Christ Beta 2-8 LD plus) for 24 h in order to allow the formation of a 3D porous structure by sublimation, resulting in a nanocomposite scaffold with an interconnected network of pores. After freeze drying, composite layers were cut into predetermined sizes (scaffolds with 5 mm diameters). Finally, the nanocomposites were immersed in a bath of glutaraldehyde (GA) (Merck) solution 1% for 24 h. Treatment by the GA cross-linking agent enhanced the consistency of the scaffold network .In order to remove the residual GA, the nanocomposites were intently washed with water (Fig. 1).

Fourier transform infrared spectroscopy (FTIR)

The scaffolds were examined by Fourier transform infrared spectroscopy (FTIR), based on the identity of transmission bands associated with the vibration of functional groups (Bomem MB 100 spectrometer). Briefly, a 1 mg sample of the powdered scaffolds was carefully mixed with 300 mg of KBr and pelletized under vacuum. The resulting pellets were subsequently analyzed in the 400–4,000 cm^{-1} range.

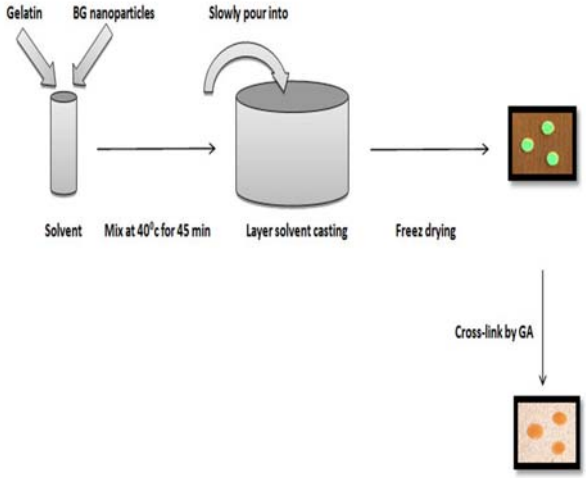

Fig 1: A schematic depicting the fabrication process of hybrid nanocomposite scaffolds

Scanning electron microscopy (SEM)

Scanning electron microscopy (SEM) was used to evaluate the morphology and microstructure, and measure the pore size of the nanocomposite scaffolds. Dry nanocomposite scaffolds were sputter-coated with a thin layer of gold (Au) (EMITECH K450X, England), and then analyzed by a scanning electron microscope(SEM-Philips XL30) operating at an accelerating voltage of 15 kV.

Cytotoxicity evaluation

Nanocomposite scaffolds were sterilized after being immersed in 70% ethanol for 1 h. They were then placed inside a standard 6-well polystyrene (PS) plate, and washed with sterile distilled water, followed by sterile phosphate buffered saline (PBS) solution and nally culture medium. Then, Dulbecco's modied Eagle's medium (DMEM) (Gibco), containing 15% fetal bovine serum (FBS) (Gibco) and 100 U/ml penicillin-streptomycin (P/S) (Gibco), was added to the PS plates. Rat mesenchymal stem cells were added to each of the wells at a density of 4×10^5 cells mL^{-1}, and were then maintained in an incubator (37 ^{0}C, 5 % CO_2) for 48 h [11,12]. Finally, the samples were xed in 100 % ethanol for 15 min, and visualized by light microscopy (Nikon Eclipse 50i) [13].

Thiazolyl blue tetrazolium bromide (MTT) detection of viable cells

The MTT assay is a simple colorimetric assay that is used for the quantification of live cells [14, 15]. The cytotoxic effects of the nanocomposite scaffolds were evaluated using the MTT assay. Rat mesenchymal stem cells were seeded in 96-well culture plates at a density of 1.7×10^4 cells $well^{-1}$. The cells were cultured in DMEM culture medium containing 10 % FBS and 100 U/ml penicillin-streptomycin, and allowed to incubate under a 5 % humidified CO_2 atmosphere, at 37 ^{0}C for 24 h. After 90% confluency, The culture media were removed and added

to the medium that had interacted with the scaffolds. After 72 h, 100 µl of fresh medium and 13 µl of MTT solution [3-(4,5-Dimethylthiazole-2-yl) -2,5-diphenyltetrazolium bromide] were further diluted into DMEM without phenol red. The resulting solution was added to each of the wells, after which media were removed. Following 4 h of incubation in the dark at 37 ^{0}C, media were removed and 100 µl of dimethyl sulfoxide (DMSO, Sigma-Aldrich, Germany) was added to each well on the plate, so as to dissolve formazan crystals. The well without a scaffold was used as a negative control. The optical density of the solution was measured at 570 nm on an ELISA plate reader (Tecan, Switzerland).

Cultivation of Mesenchymal stem cells

Bone marrow was obtained from 6-8 weeks - old Wistar rats. The animals were killed by cervical dislocation, and their tibias and femurs were dissected and cleaned of all soft tissue. The epiphysis of each bone was clipped, and the bone marrow was ushed out of the tibia and femur, and suspended in DMEM .The resulting cell suspensions were then combined and centrifuged at 1200 g for 5 min. The pellet was subsequently resuspended in fresh primary medium [DMEM supplemented with 15% FBS and 100 U/ml of penicillin-streptomycin], and used to seed tissue culture flasks , which were then incubated at 37^{0}C in a humidified incubator at an atmosphere of 5% CO_2. After three days of expansion, the cultures were rinsed three times with PBS to remove non-adherent cells. The medium was exchanged every three days throughout the studies. For use in the ensuing experiments, adherent cells were rinsed thoroughly with PBS and then detached by trypsinization (trypsin – EDTA) (Gibco).

Osteogenic differentiation of MSCs

Osteogenic differentiation was induced by culturing confluent rat MSCs for 3 weeks in inducing medium, as described previously [16].The inducing medium was a complete medium supplemented with 10 nM dexamethasone (Sigma Aldrich, Germany), 50 µg/ml of L-ascorbic acid-2-phosphate (Sigma – Aldrich), and 10 mM â glycerophosphate (Sigma Aldrich). The osteogenic medium was changed three times a week . After 28 days, occurrence of differentiation was examined by alizarin red staining and RT-PCR analysis. Using alizarin red histochemistry, the cultured cells were stained on day 28 to assess the mineralized matrix. The medium was removed, and the cell layers were rinsed 3 times with PBS and then allowed to air dry. The fixed cells were stained with alizarin red S (pH 7.2) (BIO-IDEA, Iran). After 1 h, the cell layers were washed with deionized water and observed with under a light microscope (Nikon Eclipse 50i).

RNA extraction and RT – PCR analysis of gene expression

Total RNA was purified from osteoblasts differentiated in osteogenic medium, by using the TRIpure reagent (Roche). Reverse transcription – polymerase chain reaction (RT-PCR) analysis was performed to identify the marker genes 28 days after differentiation; these were osteocalcin and osteopontin. Standard reverse transcription reactions were performed using the First Strand cDNA Synthesis Kit (Bioneer, Korea), in accordance with the manufacturer's instructions. Primer sequences and details are summarized in Table 1. Consequently, the cDNA product was amplified by PCR using a thermocycler (Eppendorf, USA). The PCR-amplified products were resolved on 1.5% agarose gel electrophoresis and then visualized by ethidium bromide staining.

Cell seeding on scaffold

Briefly, gelatin /nano-bioglass scaffolds were sterilized using 70% ethanol, and then rinsed several times with PBS [17]. The rMSCs were released from the culture substratum during the third passage using trypsin/EDTA, and were suspended in DMEM medium without FBS. Thereafter, the rMSCs were seeded onto the scaffolds by pipetting the cell suspension onto the materials. The resulting rMSCs/ scaffold construct was incubated for an additional 4 h to allow cell attachment in vitro before implantation. The extent of cell attachment and growth was assessed 24 h and 5 days after cell seeding. The constructs were fixed in 2.5% GA for 1 h at room temperature. After thoroughly washing with PBS, the cells had adhered to the scaffold section, which was then dehydrated in an ethanol – graded series (50-100%) for 5 min each, and allowed to dry on a clean bench at room temperature [4]. The samples were subsequently characterized by SEM following gold coating.

Surgery and transplantation procedure

Before performing animal surgery, the gelatin / nano-bioglass scaffolds (5 mm in diameters, full thickness) were sterilized using 70% ethanol, and then rinsed several times with PBS [17]. The rMSCs were then seeded onto the scaffolds by pipetting the cells suspension onto the materials. All surgery was performed in accordance with the Ethics Committee at Baqiyatallah University of Medical Sciences regarding the protection of animals used for experimental and other scientific purposes. In the present study, 24 adult male Wistar rats (Pasteur Institute of Iran), aged 3 to 4 months and weighing 200 to 300 g, were used. Two groups of study were formed, with 12 rats being assigned to group A and 12 to group B

Table 1: List of the primer names and sequences used in the experiments

Gene name	Forward	Reverse	Reference	Anealing temperature
Osteocalcin	GTCCCACACAGCAACTCG	CCAAAGCTGAAGCTGCCG	-	58C
Osteopontin	AGCAGGAATACTAACTGC	GATTATAGTGACACAGACTATT	32	48C

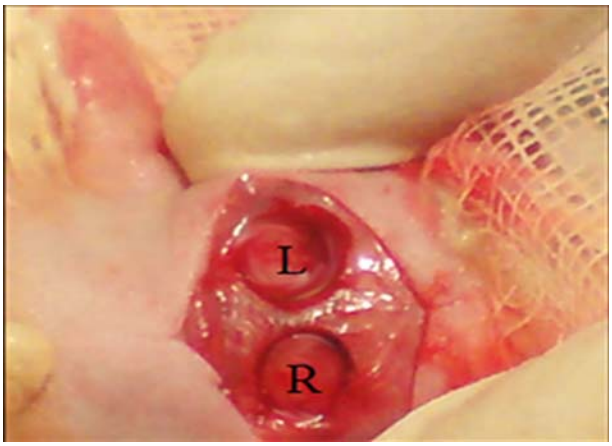

Fig 2:Intraoperative view of the rat skull after drilling the defect holes to fill with blank scaffold (L) and rMSC – scaffold construct (R)

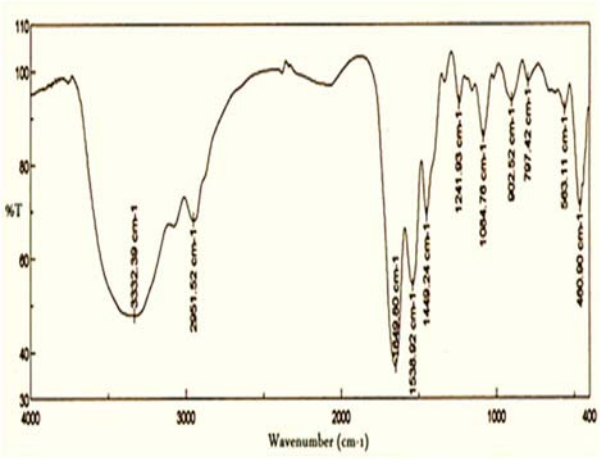

Fig 3: FTIR spectra of the nanocomposite scaffold cross – linked by GA

representing the control group (see Table 2). The animals were anesthetized by a combination of ketamine (25 mg/g) and xylazine (2.5 mg/g). Then, skin and underlying tissues of the vertex, were raised to expose the calvaria, and two defects (5 mm in diameter-a critical size [17]), in symmetry to the sagittal suture, were generated using a trephine bur in each animal, under constant irrigation with 0.9% physiologic saline. The procedure was performed under sterile conditions. After the bone was removed, the defects in the left side and the right side of calvaria were grafted with the blank scaffold and rMSCs/scaffold construct, respectively. Thereafter, the skin incision was closed with silk sutures (Fig. 2).

Radiographic evaluation

After surgery, rats were sacrificed at 4, 6, 8 and 12 weeks after transplantation, and their calvarial grafts were harvested. The calvarial defects were then allowed to heal by a radiological procedure to monitor the placement of the graft and the bony integration. The percentage of newly formed bone was measured in the radiographs using Scion Image software. The percentage of healing was calculated as follows [8]:

% healing = area of the defect filled with new bone)/(area of the original defect)

Histological evaluation

For histological examination, at 4, 6 and 12 weeks after implantation, the rats were sacrificed and the implants were individually dissected. The harvested samples were immediately fixed in 10% formalin, decalcified in 5% nitric acid (Merck), and then embedded in sucrose (10, 20 and 30%). The sections were cut to a thickness of 10 µm using a freezing microtome, and then mounted onto glass slides, and stained with hematoxylin and eosin (H&E) using standard methods, as described previously [18,19]. The sections were then observed and photographed with a microscope (Nikon SMZ 1500, Japan).

Results

FTIR analysis

The FTIR spectra obtained from scraped material surfaces, recorded after the synthesis of the nanocomposite scaffolds, in the 400-4000 cm^{-1} spectral range, are shown in Figure 3 . In the nanocomposite spectrum, five characteristic transmission bands relating to gelatin and BG at the frequencies of 1260, 1560, 1670, 2952 and 3570 cm^{-1} could be observed. The most characteristic spectra were those belonging to proteins, where the amide III bands originated from the N-H bending vibration at 1260 cm^{-1}, the amide II bands was caused by the N-H bending vibration at 1560 cm^{-1}, the amide I bands originated from the C = O stretching vibration at 1670 cm^{-1}, and the C – H bending vibration at 2952 cm^{-1} was for amide B, and the band at 3570 cm^{-1}indicated the presence of O – H groups [20,21]. The other two bands were the result of chemical bonds that were

Table 2: List of the treatment groups of experimental animals

Group	Rat number		Graft at left defect	Graft right defect	Control
	Group A: 5 mm diameter	Group B: control			
4 weeks	3	3	Blank scaffold	rMSC construct	Blank defect
6 weeks	3	3	Blank scaffold	rMSC construct	Blank defect
8 weeks	3	3	Blank scaffold	rMSC construct	Blank defect
12 weeks	3	3	Blank scaffold	rMSC construct	Blank defect

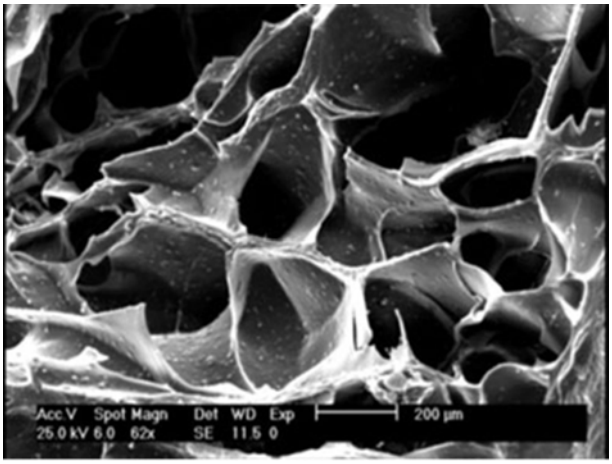

Fig 4: SEM micrograph from the surface of the synthesized BG/GEL nanocomposite scaffold

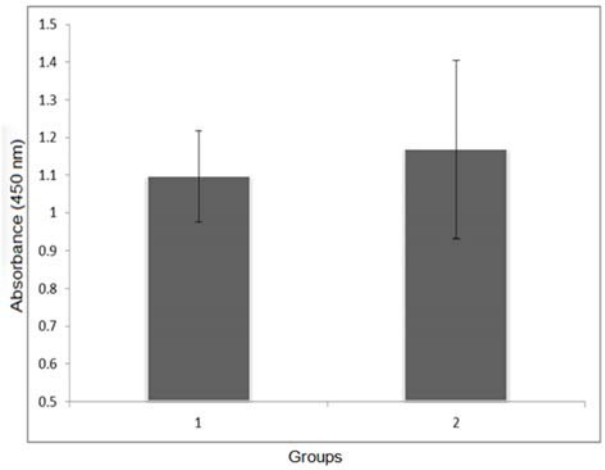

Fig 5: Micrograph of the mesenchymal stem cells grown on the scaffolds cross-linked with 1% GA (rMSC: rat mesenchymal stem cell, S: scaffold) (100 X)

formed due to the mixing of BG with Gel, and then cross-linking with GA. The peak related to the bond between the Gel (carboxyl groups) and BG (Ca^{2+}) appeared at 1345 cm^{-1}. After cross-linking of the Gel with GA, the second peak appeared at 2363 cm^{-1} [20].

SEM observations

The morphology of scaffolds, as revealed by SEM micrographsin Figure 4 , indicated a network of interconnected pores with a smooth surface morphology and fairly uniform spherical shape. The diameter of the pores in the nanocomposite samples ranged from 250 to 500 µm, which is desirable for bone cell growth [9,10,22,23].

Cytotoxicity evaluation

Indirect cytotoxicity test was carried out on rat mesenchymal stem cells, 48 h after exposing them to the scaffolds. The cytotoxic effects of the scaffolds on rMSCs, is distinguished because of the observation of cellular attachment, development of filopodias, dispersion and formation of monolayers. These results indicate that the scaffolds are suitable for the support of cell growth (Fig. 5).

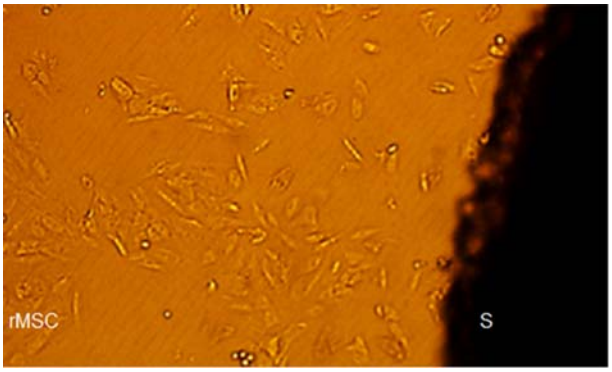

Fig 6: Cell viability evaluated by the MTT assay after 72 h. Groups 1 and 2 indicate test and negative control samples, respectively

MTT detection of viable cells

MTT assays were performed to assess mitochondrial activity and observe the cytotoxic effects of the scaffolds on rat MSCs in vitro. The results indicated that the scaffolds were not toxic to rMSCs, based on the comparison of data from the test and the control (Fig. 6).

Cell culture

A small portion of the nucleated cells introduced into the culture were marrow – derived mesenchymal cells . The remainder of the cell population, containing various types of non-adherent hemopoietic cells , were removed on the fifth day of cultivation by replacing the existing medium with fresh medium. Adherent marrow – derived mesenchymal cells were shown to have similar fibroblastic morphology, while others were found to be round with dark centers and transparent peripheries. In the early stages of cultivation, the adherent cells were seen as individual cells (Fig .7 a). However, in the subsequent days, they proliferated rapidly, forming colonies of up to 100 pure fibroblastic cells. At the end of the second week, colonies of fibroblastic mesenchymal cells had expanded in size; with some small round cells appearing in the colonies (Fig.7 b) .When the cell density within the colonies reached 80 to 90% confluency, each primary culture was passaged onto new plates, so as to prevent the mesenchymal cells from slowing their rate of division or differentiation (Fig.7c). At the third passage, these cells had been completely obscured by the fibroblastic cells.

Osteogenic differentiation of MSCs

After 28 days of cultivation in osteoinductive medium, nodule – like structures had appeared in certain areas of

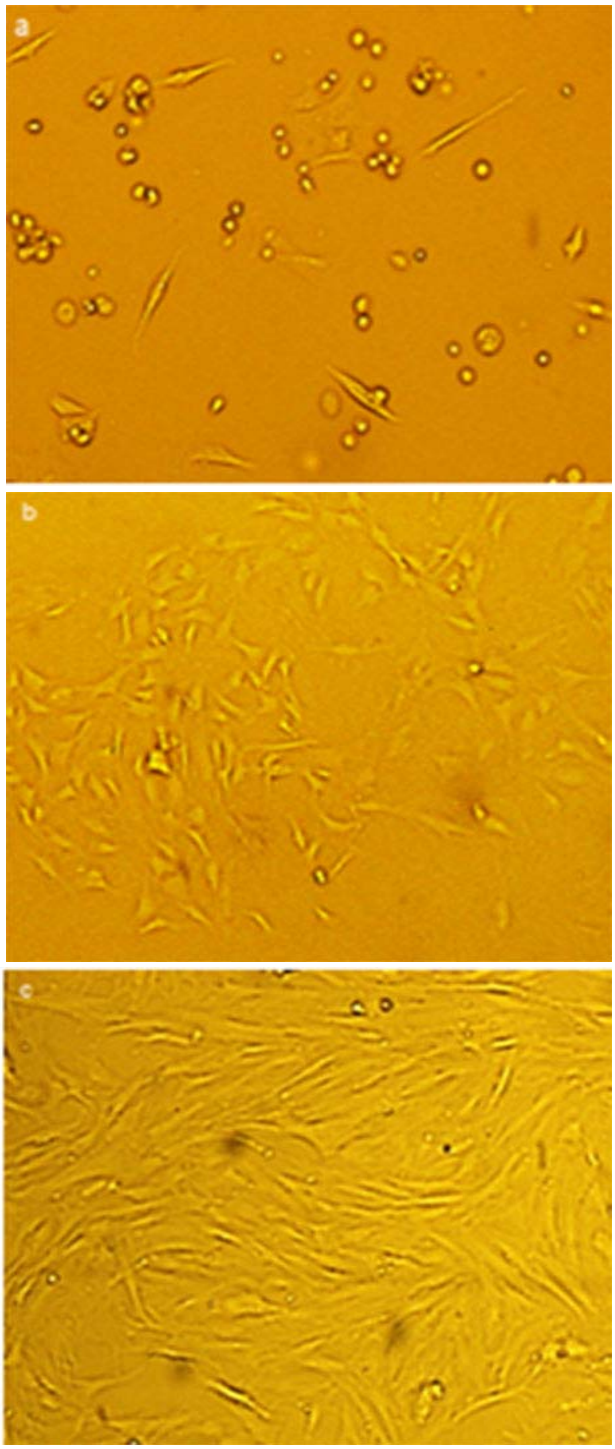

Fig 7: Rat bone marrow culture. (a) after the first culture medium change on day 3 of cultivation, the adherent cells are seen as individual cells, (b)on day 14 of primary cultivation, some round cells have appeared on the fibroblastic clones, and (c) pure fibroblastic monolayer (100 X)

the culture plate. But only a few cells had become detached and floated in the culture medium. Following alizarin red staining, the stain for bone nodule formation was positive, as indicated by the red mineralized areas of the culture (Fig. 8). Differentiation was further demonstrated by RT – PCR analysis of bone related genes. RT-PCR analysis showed that bone specific proteins including osteopontin and osteocalcin were expressed in the cells. These data indicated that bone differentiation occurred in the culture of the purified cells (Fig. 9).

Cell seeding on scaffold

The ability of the scaffolds to support cell growth and cellular attachment was evaluated by SEM. The SEM images of rMSCs cultured on the nano bioglass scaffolds are shown in Figure 10. Twenty four hours after cell seeding, the rMSCs became attached to the inner surface of the scaffolds. After incubation of for 5 days, the cells, which had grown tightly attached to each other, were suspended among the backbones of the scaffolds and had grown along the pores of the scaffolds. Moreover, cells that reached confluence, formed abundant fibril networks of extracellular matrix that were deposited on the scaffolds. These results indicated that the nanocomposite scaffold was suitable for supporting the growth of cells.

Radiographic evaluation

To evaluate new bone formation and the ability of the BG scaffolds seeded with rMSCs, to heal critical-sized defects in rat calvaria, X-ray images were taken at 4, 6, 8 and 12 weeks post-implantation (Fig. 11).The new bone formation and mineralization in the full- thickness defect were observed on the right side of calvaria, while the defect on the left side had healed to a lesser extent at 8 and 12 weeks post-implantation. The defect in the control group failed to show any appreciable new bone formation. Moreover, the volume and area of the BG scaffolds were seen to decrease, when the implantation time was increased from 4 to 12 weeks. These results demonstrated that BG scaffolds, enhanced with rMSCs, can efficiently improve the speed of the bone healing process in an allograft transplantation model, when compared to other groups. In addition, based on the results of the bone reconstruction percentage analysis (densitometry), there was a significant difference in new bone formation percentage between the area grafted with blank scaffold and the area grafted with rMSCs construct (Fig.12).

Histological evaluation

The process of bone reconstruction in the calvaria, with a critical defect size of 5 mm, was evaluated by histological analysis. Photomicrograph of calvaria revealed the healing process in both groups (Fig. 13). Four weeks after implantation, the scaffold was invaded by blood cells and showed a granulation tissue pattern with a residual clot component. Some residual scaffold materials were scattered in the graft area (Fig.13a, b). After 6 weeks post-implantation, the scaffold had decreased in weight and volume, because of its biodegradable property (Fig. 13c, d). However, after 12 weeks post-implantation with the rMSC/scaffold

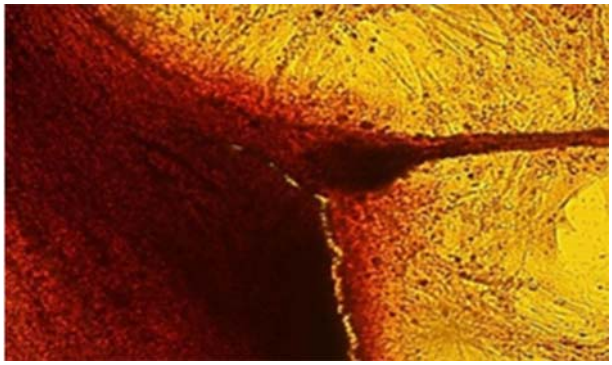

Fig 8: MSCs have differentiated into mineralizing cells stained with alizarin red, showing red mineralized areas of culture (100 X)

component, various amounts of bone formation were observed between the intact bone and the scaffold (Fig .13 f, 14). However, in the case of the blank scaffold implantation, only a little ossification was observed (Fig.13 e). The micrograph of the control group at 12 weeks post-implantation indicated the presence of a thin membrane in the defect area without any graft (Fig.13 g).

Discussion

Osteoconductive scaffolds and osteoprogenitor cells are the two main factors that are involved in bone tissue regeneration. The main challenge during the repair and reconstruction of bone defects is the search for biocompatible and functionally proven graft materials [24]. The current research investigated the ability of a gelatin / nano-bioglass scaffold to support the differentiation and viability of rMSCs and repair of critical cranial bone defects. The BG nanocomposite scaffolds are biodegradable, osteoconductive and biocompatible , and perform the role of a temporary matrix for cells to grow on and differentiate [3, 25]. Mesenchymal stem cells derived from the bone marrow are adherent cells of non-hematopoietic origin that have a strong regeneration and multi-lineage differentiation potential, and immunosuppressive properties that are important for cell therapy and allografts [17].

In this study, BG nanocomposite scaffolds were fabricated by layer solvent casting combined with freeze drying. In order to study chemical bonds in the BG nanocomposite construct, FTIR analysis of the nanocomposites were carried out. Results indicate that there are certain connections at the molecular level, beyond the nanocomposites components, that are primarily due to of the BG-gelatin mixture. The band located at 1345 cm^{-1} is attributed to bond formation between Ca^{2+} ions in BG and the COOH groups in gelatin. In fact, the presence of such bonds between the nanocomposite components is the reason behind the enhanced mechanical properties of this type of scaffold, when compared to those of the conventional composite scaffolds [11, 22]. Additionally, a band at 2349 cm^{-1} appeared after cross-linking of gelatin with GA that is attributed to C – H bond in the C_3H_6 molecule, which is a residue of the reaction between GA and gelatin chains [22]. Scanning electron microscopy was used to observe the average pore diameter of the nanocomposite scaffolds.

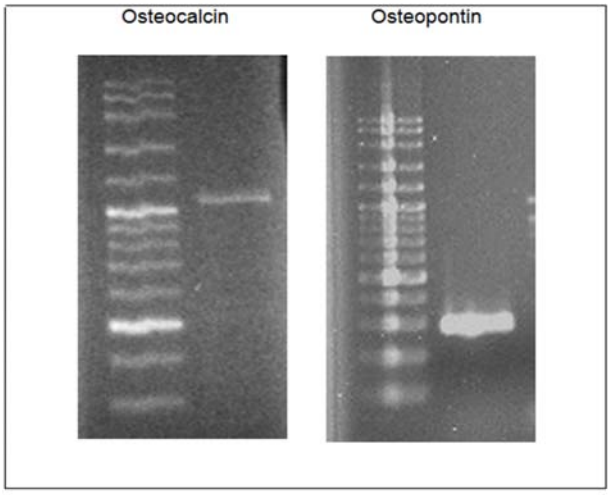

Fig 9:RT – PCR analysis. Mineralized cells expressing osteocalcin, osteopontin and alkaline phosphatase

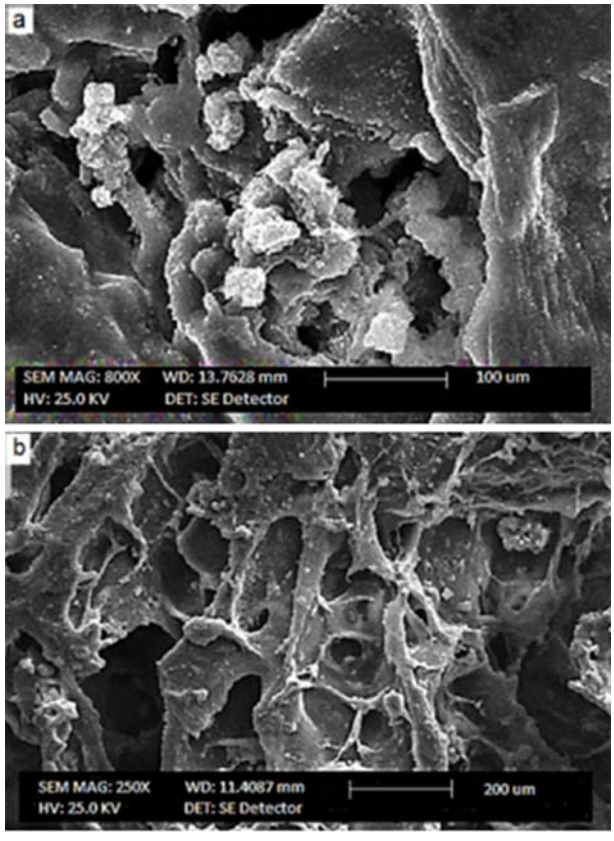

Fig 10: SEM micrographs of rMSCs cultured on the nanocomposite scaffolds. (a) 24 h and (b) 5 days after cell seeding

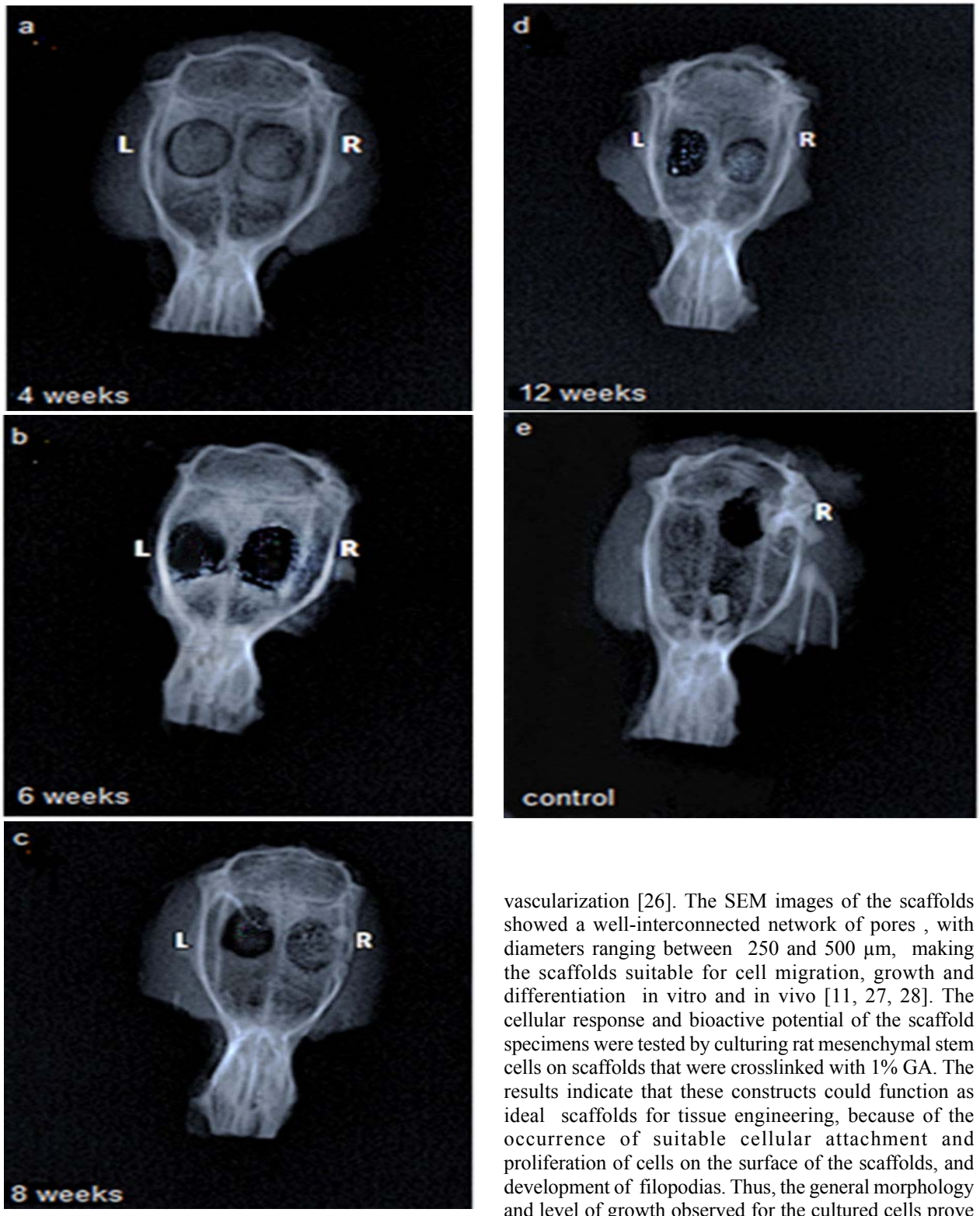

Fig 11: Radiographic evaluation of the repaired calvaria, (a-e) typical radiographs of the defect site at (a) 4 weeks, (b) 6 weeks, (c) 8 weeks, and (d) 12 weeks after the implantation; (e) control group

It is very important and highly critical that the pore size in the engineered scaffold be greater than 100 µm, so as to allow cellular migration, tissue ingrowth and ultimately, vascularization [26]. The SEM images of the scaffolds showed a well-interconnected network of pores , with diameters ranging between 250 and 500 µm, making the scaffolds suitable for cell migration, growth and differentiation in vitro and in vivo [11, 27, 28]. The cellular response and bioactive potential of the scaffold specimens were tested by culturing rat mesenchymal stem cells on scaffolds that were crosslinked with 1% GA. The results indicate that these constructs could function as ideal scaffolds for tissue engineering, because of the occurrence of suitable cellular attachment and proliferation of cells on the surface of the scaffolds, and development of filopodias. Thus, the general morphology and level of growth observed for the cultured cells prove that they could survive and function normally on the scaffolds. The results obtained from the MTT assays showed the absence of cytotoxic effects on the viability and proliferation properties of cells, after 72 h.

This result suggested that the BG nanocomposite scaffold is not toxic to cells and is therefore, a suitable candidate for use as a bone scaffold [29].In the present investigation, the mesenchymal stem cells, possessing a multi-lineage

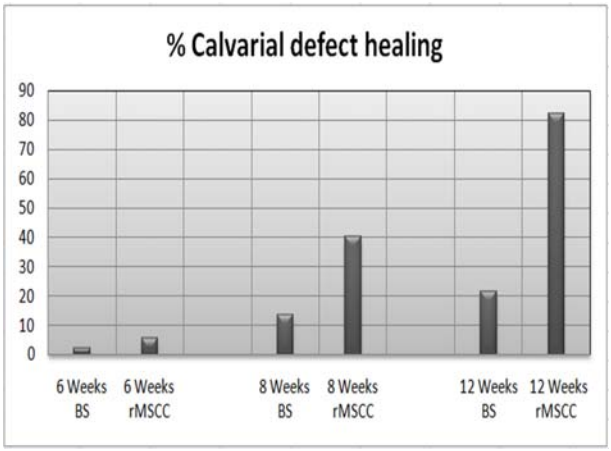

Fig 12: Bone regeneration percentage of the defect area at 6,8 and 12 weeks after implantation. The six bars represent the different bone regeneration ability of blank scaffold and rMSCs construct. A statistically significant difference was shown between blank scaffold and rMSCs construct (BS: Blank Scaffold, rMSCC: rat Mesenchymal Stem Cell Construct).

differentiation capability, were isolated from rat bone marrow. Certain features of the MSCs, having been isolated, confirmed their identity. Furthermore, the most important properties of such cells include multi-lineage mesenchymal differentiation in appropriate medium, as demonstrated by alizarin red staining and RT-PCR analysis [30]. In the osteoinductive cultures, alizarin red staining showed the presence of bone nodule formation, as indicated by red mineralized areas on the culture [30, 31]. Also, RT – PCR studies revealed the expression of the osteogenic markers, osteocalcin and osteopontin. This evidence together with the fibroblastic morphology of the cells suggested that they must be mesenchymal stem cells [30]. To evaluate the ability of the scaffolds to support cell growth, cellular attachment and interaction within 3D scaffolds, the rMSCs were seeded onto the BG scaffold and monitored by SEM.

Results showed that the BG scaffolds have pores with a suitable diameter for cell seeding and growth. In addition, the cells, after being cultured in vitro, were found attached along the material surface, actively secreting extracellular matrix [3,7]. For the in vivo study, rat calvarial defects, each with a diameter of 5mm, were used to investigate bone repair, because such a defect size is beyond the size of spontaneous bone regeneration [17]. An empty defect was used as a control, and the BG scaffold, with and without rMSCs, was implanted at the calvarial defect in the rat, to assess the positive effects of rMSCs on the bone reconstruction of rat calvaria. According to radiographic and densitometry analysis, new bone

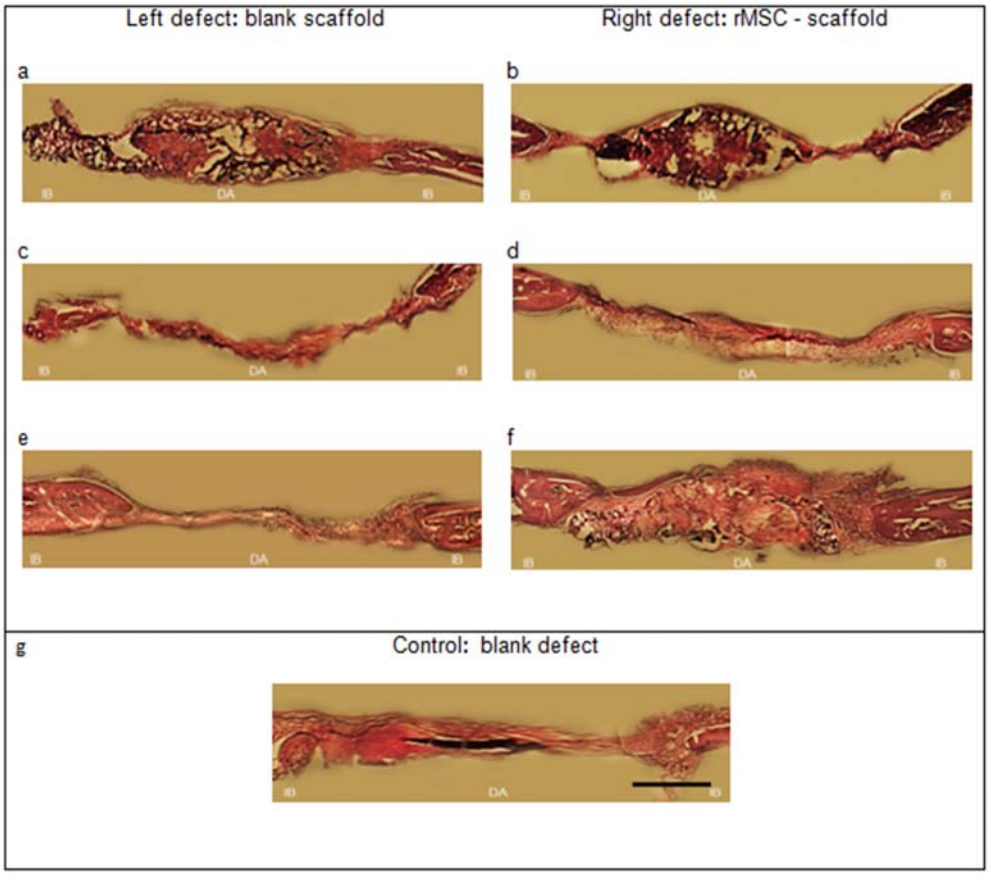

Fig 13: Histological analysis of new bone formation. Defect areas were treated with (a, c, e) blank scaffold and (b, d, f) rMSC/scaffold construct in 4, 6 and 12 weeks, after transplantation. (g) Blank defect in 12 weeks. (IB: Intact bone, DA: Defect area), scale bar=1cm

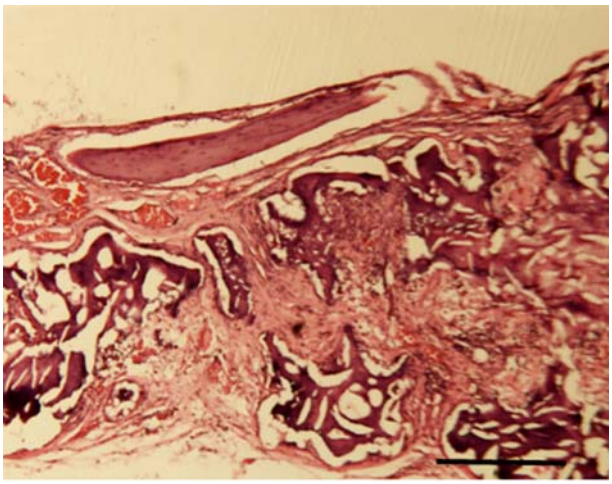

Fig 14: Histological analysis of calvarial defects filled with rMSC/scaffold construc, 12 weeks after implantation, scale bar=0.5 cm

formation in the area grafted with the rMSCs/scaffold construct was superior to that in the area grafted with a blank scaffold.

In contrast, the empty defect failed to show any appreciable new bone formation and needed much more time to regenerate. Histological analysis also showed the same pattern of bone healing, as demonstrated by radiological assessment. Invading blood cells fill the scaffold during the early stages of repair. Twelve weeks after implantation, trabecular and cortical bone formation were observed, in contrast to the control and blank scaffold groups, where bone repair did not occur.

Conclusion

In summary, the in vitro results showed that the gelatin/nano-bioglass scaffolds were biocompatible, and cells seeded onto these scaffolds attached to the pore walls. Also, according to radiographic evaluation and histological analysis, the combination of nanocomposite scaffolds with rMSCs further enhanced new bone formation. Thus such a composite could have superior potential in bone regeneration, when compared to the blank scaffold. Therefore, the present research provides data which can support the future use of gelatin/nano-bioglass scaffolds with rMSCs in bone repair.

Acknowledgments

This work was supported by the Iran National Science Foundation (INSF) and Division of Tissue Engineering, Baqiyatallah University Of Medical Sciences Tehran, Iran. The authors would like to thank Dr. Mohammad Hossein Abnoosi (Department of Biology, University of Arak, Iran) for his kindly cooperation in cell culture techniques.

References

1. M Azami, F Moztarzadeh, M Tahriri. Preparation, characterization and mechanical properties of controlled porous gelatin/hydroxyapatite nanocomposite through layer solvent casting combined with freeze-drying and lamination techniques. J Porous Mater, 17, 313-320 (2010).
2. M Azami, M Rabiee, F Moztarzadeh. Glutaraldehyde crosslinked gelatin/hydroxyapatite nanocomposite scaffold, engineered via compound techniques. J Polym Compos,31,2112-20 (2010).
3. M Azami, S Tavakol, A Samadikuchaksaraei, M Solati Hashjin, N Baheiraei, M Kamali, MR Nourani. A porous hydroxyapatite/gelatin nanocomposite scaffold for bone tissue repair:In vitro and In vivo evaluation. Journal of Biomaterials, 1-17 (2012).
4. M Bghaban Eslaminejad, H Nazarian, L Taghiyar. Mesenchymal stem cell isolation from the removed medium of rat's bone marrow primary culture and their differentiation into skeletal cell lineages. Yakhteh Medical Journal, 65-72 (2008).
5. M Baghaban Eslaminejad, A Nikmahzar, L Taghiyar, S Nadri, M Massumi. Murine mesenchymal stem cells isolated by low density primary culture system. Develop. Growth Differ, 361-370 (2006).
6. D Ben-David, T A.Kizhner, T Kohler, R Muller, Livne E, Srouji S. Cell-scaffold transplant of hydrogel seeded with rat bone marrow progenitors for bone regeneration. Journal of Cranio-Maxillo-Facial Surgery, 364-371 (2011).
7. J.J Chen, H Jin, D.M Ranly, J Sodek, B.D Boyan. Altered expression of bone sialoproteins in vitamin D-deficient rBSP2.7Luc transgenic mice. J Bone Miner Res, 14:221 (1999).
8. C.J Damien, J.R Parsons. Bone graft and bone graft substitutes: a review of current technology and applications. J Appl Biomater, 2,187-208 (1991).
9. A Doostmohammadi, A Monshi, Ret al Salehi. Cytotoxicity evaluation of 63S bioactive glass and bone-derived hydroxyapatite particles using human bone-marrow stem cells. Biomed Pap Med Fac Univ Palacky Olomouc Czech Repub. 155, 323-6 (2011).
10. C E.Petric Aronin, K W.Sadik, A L.Lay, D B.Rion, S S.Tholpady, R C.Ogle, E A.Botchwey. Comparative effects of scaffold pore size,pore volume, and total void volume on cranial bone healing patterns using microsphere-based scaffolds. J Biomed Mater Res, 89, 632-641 (2009).
11. L Fassina, E Saino, L Visai et al., Use of a gelatin cryogel as biomaterial scaffold in the differentiation process of human bone marrow stromal cells . Conf Proc IEEE Eng Med Biol Soc, 247-50 (2010).
12. F Hafezi ,F Hosseinnejad, A A Imani Fooladi, S Mohit Mafi, A Amiri, M R Nourani. Transplantation of nano-bioglass/gelatin scaffold in a non-autogenous setting for bone regeneration in a rabbit ulna. J Mater Sci: Mater Med. 23, 2783-92 (2012).
13. F Hosseinnejad, A.A Imani Fooladi, F Hafezi, S Mohit Mafi, A Amiri, M R Nourani. Modeling and tissue engineering of three layers of calvarial bone as a biomimetic scaffold. Journal of Biomimetics, Biomaterials & Tissue Engineering, 37-53 (2012).
14. DW Hutmacher. Scaffolds in tissue engineering bone and cartilage. Biomaterials, 2529-2543 (2000).
15. A.A Imani Fooladi, H Mahmoodzadeh Hosseini, F Hafezi, F Hosseinnejad, M R Nourani. Sol-gel derived bioactive glass containing SiO2-MgO-CaO-P2O5 as an anti-bacterial scaffold. J Biomed Mater Res,344-64 (2012).
16. X Jiang, J Zhao, S Wang, X Sun, X Zhang, J Chen, D L.Kaplan, Z Zhang. Mandibular repair in rats with premineralized silk scaffolds and BMP-2-modified bMSCs. J Biomaterials, 30 , 4522-4532 (2009).
17. S.N Khan, F.P Cammisa Jr, H.S Sandhu, A.D Diwan, F.P Girardi, J.M Lane. The biology of bone grafting. J Am Acad Orthop Surg, 13, 77-86 (2005).
18. H.S Mansur, H.S Costa. Nanostructured poly (vinyl alcohol)/bioactive glass and poly (vinyl alcohol)/chitosan/bioactive glass hybrid scaffolds

for biomedical applications. Chem Eng J, 137, 72-83 (2008).
19.Miao, T.M.O.S.A.X. Preparation and characterisation of plga-coated porous bioactive glass-ceramic scaffolds for subchondral bone tissue engineering. Ceramic Transactions (2008).
20. J.L Milan , A Josep, P Lacroix. Simulation of bone tissue formation within a porous scaffold under dynamic compression. Biomech Model Mechanobiol, 9, 583-96 (2010).
21. M Mozafari, M Rabiee, M Azami, S Maleknia. Biomimetic formation of apatite on the surface of porous gelatin/bioactive glass nanocomposite scaffolds. J Applied Surface Science, 1740-9 (2010).
22. J Picot, editor. Human cell culture protocol. New Jersey: Humana Press (2004).
23. I R.Degano, M Vilata, J R.Bago et al. Bioluminescence imaging of calvarial bone repair using bone marrow and adipose tissue-derived mesenchymal stem cells. J Biomaterials, 427-437 (2007).
24. A.J Salgada, O.P Coutinho, R.L Reis. Bone tissue engineering:state of the art and future trends, macromol. Biosci, 743-765 (2004).
25. M Sila-Asna, A Bunyaratvej, S Maeda, H Kitaguchi, N Bunyaratavej. Osteoblast differentiation and bone formation gene expression in strontium-inducing bone marrow mesenchymal stem cell. Kobe J. Med. Sci.25-35 (2007).
26. S.R Stock. X-ray microtomography of materials. Int Mater Rev, 44, 141-64 (1999).
27. J.T Tian, J.M Tian. Preparation of porous hydroxyapatite. J Mater Sci, 36, 3061-6 (2001).
28. Q TU, P Valverde , S LI, J Zhang, P Yang, J Chen. Osterix overexpression in mesenchymal stem cells stimulates healing of critical-sized defects in murine calvarial bone. J Tissue Eng, 13, 2431-2440 (2007).
29. J.H Ye, Y.J Xu, J Gao et al. Critical-sized calvarial bone defects healing in a mouse model with silk scaffolds and SATB2-modified iPSCs. J Biomaterials, 2011;5065-5076.
30. J.H Zhang, J Wang, J Tang et al. Bone sialoprotein promotes bone metastasis of a non-bone seeking clone of human breast cancer cells. Anticancer Res. 24,1361-8 (2004).
31. X Zhang, T Tang, Q Shi, J C.Fernandes, K Dai. The immunologic properties of undifferentiated and osteogenic differentiated mouse mesenchymal stem cells and its potential application in bone regeneration. J Immunobiology, 179-186 (2008).
32. C Zong, D Xue, W Yuan et al. Reconstruction of rat calvarial defects with human mesenchymal stem cells and osteoblast-like cells in poly-lactic-co-glycolic acid scaffolds. European Cells and Materials, 109-120 (2010).